

# Multimodal Classification and Out-of-distribution Detection for Multimodal Intent Understanding

Hanlei Zhang\*, Qianrui Zhou\*, Hua Xu, *Member, IEEE*, Jianhua Su, Roberto Evans, Kai Gao

**Abstract**—Multimodal intent understanding is a significant research area that requires effectively leveraging multiple modalities to analyze human language. Existing methods face two main challenges in this domain. Firstly, they have limitations in capturing nuanced and high-level semantics underlying complex in-distribution (ID) multimodal intents. Secondly, they exhibit poor generalization when confronted with unseen out-of-distribution (OOD) data in real-world scenarios. To address these issues, we propose a novel method for both ID classification and OOD detection (MIntOOD). We first introduce a weighted feature fusion network that models multimodal representations effectively. This network dynamically learns the importance of each modality, adapting to multimodal contexts. To develop discriminative representations that are conducive to both tasks, we synthesize pseudo-OOD data from convex combinations of ID data and engage in multimodal representation learning from both coarse-grained and fine-grained perspectives. The coarse-grained perspective focuses on distinguishing between ID and OOD binary classes, while the fine-grained perspective enhances the understanding of ID data by incorporating binary confidence scores. These scores help to gauge the difficulty of each sample, improving the classification of different ID classes. Additionally, the fine-grained perspective captures instance-level interactions between ID and OOD samples, promoting proximity among similar instances and separation from dissimilar ones. We establish baselines for three multimodal intent datasets and build an OOD benchmark. Extensive experiments on these datasets demonstrate that our method significantly improves OOD detection performance with a 3-10% increase in AUROC scores while achieving new state-of-the-art results in ID classification.<sup>1</sup>

**Index Terms**—Multimodal intent understanding, intent classification, out-of-distribution detection, multimodal fusion.

## I. INTRODUCTION

Multimodal intent understanding is a rapidly growing field in multimodal language analysis [1]. It aims to leverage information from various modalities in real-world scenarios (i.e., text, video, and audio) to enable machines to comprehend complex semantics (e.g., intents) from human conversations. Recognizing user intents can significantly enhance service

Hanlei Zhang, Qianrui Zhou, Hua Xu, Jianhua Su and Roberto Evans are with State Key Laboratory of Intelligent Technology and Systems, Department of Computer Science and Technology, Tsinghua University, Beijing 100084, China. Jianhua Su and Kai Gao are with School of Information Science and Engineering, Hebei University of Science and Technology, Shijiazhuang 050018, China. Hua Xu is the corresponding author.

(e-mail: zhang-hl20@mails.tsinghua.edu.cn; zgr22@mails.tsinghua.edu.cn; xuhua@mail.tsinghua.edu.cn; sjh19832107090@gmail.com; linyf21@mails.tsinghua.edu.cn; gaokai@hebust.edu.cn).

\*: These authors contributed equally to this work.

This work has been submitted to the IEEE for possible publication. Copyright may be transferred without notice, after which this version may no longer be accessible.

<sup>1</sup>The full data and codes are available at <https://github.com/thuiar/MIntOOD>.

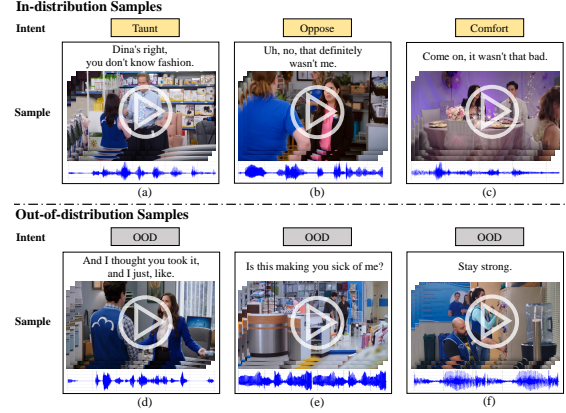


Fig. 1. Examples of in-distribution and out-of-distribution samples for multimodal intent understanding.

quality and can be applied in numerous substantial applications, such as virtual humans [2], chatbots [3], and other interaction systems [4]–[6].

However, research on multimodal intent understanding is still in its early stages, and related studies have just begun in recent years. One challenge is how to effectively perform multimodal fusion and learn representations conducive to intent classification. For example, [1] presents the first multimodal intent dataset with annotations from 20 intent categories and establishes baselines using multimodal fusion methods [7]–[9] adapted from the multimodal sentiment analysis area, demonstrating the effectiveness of non-verbal modalities in this task. [10] introduces an interaction framework that aligns video and audio with the text modality before fusing all multimodal features using a transformer. [11] proposes a prompt-based module to construct multimodal augmented pairs for token-level contrastive learning. However, these methods have limitations in learning discriminative representations to distinguish fine-grained and semantically complex intent classes.

Another challenge is that existing methods are limited to closed-world classification on in-distribution (ID) intent data and struggle with out-of-distribution (OOD) data from unseen open classes [12], [13] or irrelevant out-of-scope utterances [14], commonly encountered during conversational interactions in real-world scenarios. Figure 1 illustrates examples of ID and OOD data for multimodal intent understanding. Both ID and OOD data contain text, video, and audio modalities, and we combine these modalities to analyze the intents. Specifically, ID data come from predefined known intent classes, such as *Taunt*, *Oppose*, and *Comfort*, listed in Figures (a), (b), and (c), respectively. Though the text modality

is predominant in this task [11], non-verbal modalities often play enhancing or necessary roles. For instance, in example (a), using only the text modality might infer the speaker’s intention as *Criticize*, but analyzing the speaker’s expressions and tones from non-verbal modalities corrects it to *Taunt*. OOD data come from multimodal utterances that do not belong to existing known intents, including potential new intents, such as *Doubt* and *Encourage* in examples (e) and (f), and statements of one’s opinion as in example (d). These OOD samples are common in daily life, but most existing OOD detection methods focus on a single modality, such as vision [15], [16], text [17], [18], or leveraging one modality as prior knowledge to help the target modality for OOD detection [19], [20]. They fail to leverage multiple modalities cooperatively to generate effective representations for OOD detection. When adapting existing multimodal fusion methods to OOD detection, our experiments show they tend to overfit on ID classes and lack robustness and generalization when encountering unseen OOD samples during testing.

To address these two challenges, we propose MIntOOD, a novel method for multimodal intent classification and OOD detection. The motivation is that both tasks can be improved through effective modeling of multimodal representations and learning from discriminative information among both ID and pseudo-OOD data at multiple granularity levels. For modeling multimodal representations, we first extract feature embeddings for each modality with advanced backbones in their respective fields and then construct pseudo-OOD features of each modality through convex combinations of a certain amount of ID features from at least two different classes following the Dirichlet distribution. Next, we build encoders for each modality and design a weighted feature fusion network for effective multimodal fusion. In particular, the importance of each modality is considered by dynamically learning corresponding weights adaptive to multimodal contexts via neural networks. We perform a weighted summation on the encoded representations and normalized weights of each modality.

For learning discriminative and robust multimodal representations for both ID classification and OOD detection, we optimize the learning objectives from three perspectives. First, we use the ID and pseudo-OOD features to learn coarse-grained distinguishing characteristics by differentiating whether a sample is ID or OOD. Then, the well-trained binary classifier is used to predict each multimodal sample’s confidence scores. These scores enhance the discrimination capability among specific ID classes. We scale these scores into a broader range and multiply them with the multimodal representations, resulting in different magnitudes captured by a cosine classifier. In this way, difficult samples with lower confidence (i.e., magnitudes) receive more attention during ID classification, enhancing the ability to distinguish different ID classes. Finally, we focus on a more fine-grained granularity within instance-level ID and OOD samples. We apply contrastive learning to pull ID samples with the same class together and push away samples from different ID classes for learning ID instance interactions. When involving OOD, we force each OOD sample to separate from any other samples to enhance the model’s discrimination capability on various con-

structed OOD samples, thereby improving its generalization ability and robustness when encountering unseen OOD data.

Our contributions are summarized as follows: (1) We introduce MIntOOD, a novel method for multimodal intent classification and OOD detection. To the best of our knowledge, this is the first multimodal method that shows strong generalization ability on unseen OOD data while ensuring ID classification performance. (2) We achieve a simple and effective multimodal fusion network by fusing the encoded representations of each modality with corresponding importance degrees, through dynamically learning weight scores adaptive to multimodal contexts. (3) We design optimization objectives for learning robust representations from three different granularities, fully capturing both coarse-grained and fine-grained distinction information within ID and constructed OOD data. (4) We establish baselines for three multimodal intent datasets and create an OOD benchmark. Extensive experiments show that our method achieves new state-of-the-art performance on ID classification and significant improvements on OOD detection of 3–10% on AUROC over the best-performing baselines.

## II. RELATED WORKS

### A. Intent Understanding

Intent understanding is a significant research area, originating from natural language understanding (NLU), and aims to analyze the semantics underlying dialogue utterances, which is gaining popularity [21]. Researchers have proposed various benchmark datasets [14], [22], [23] to facilitate research progress. For these datasets, traditional supervised learning methods can achieve superior performance [24], [25]. However, it is common for OOD samples to appear during dialogue interactions, prompting research into open-world intent analysis, including open intent detection [12], [13], [26] and new intent discovery [27]–[30]. The former trains on data from ID classes and aims to recognize these known classes while also detecting unseen open classes during testing. The latter uses unsupervised or semi-supervised data to find potential intent-wise groups. However, these works only focus on the text modality and fail to leverage non-verbal modalities, which often play a crucial role in dialogue interactions.

Recently, there has been increasing interest in exploring intent understanding in multimodal scenarios. For instance, [31] introduces the MDID dataset, which combines image-text pairs from Instagram posts to analyze authors’ intents, while [32] studies market intent understanding using text and image modalities from social news. However, these tasks differ from multimodal intent analysis in conversations. [33] proposes a multimodal contextual transformer network that encodes utterances with contextual information from each modality and captures modality-specific and modality-invariant properties. The MIntRec dataset [1] makes a pioneering contribution in this area, including 2,224 multimodal utterances containing text, video, and audio modalities annotated from 20 intent categories. Moreover, it provides baselines with powerful multimodal fusion methods adapted from multimodal sentiment analysis. Based on this dataset, [10] designs a shallow-to-deep interaction module, aligning non-verbal modalities to text via

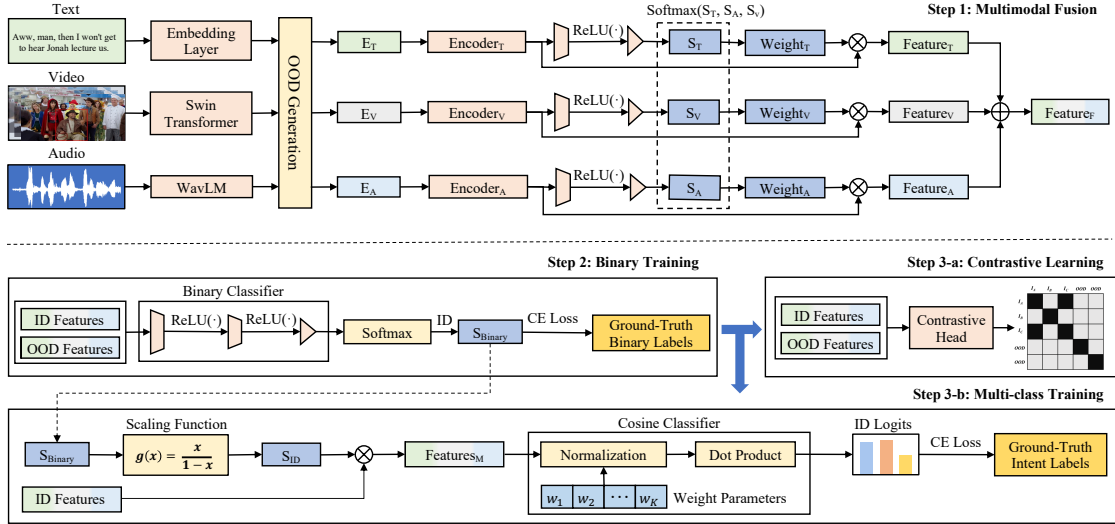


Fig. 2. Overall architecture of MIntOOD. It begins by generating pseudo-OOD samples through convex combinations of features extracted from ID samples. A weighted feature fusion network is designed to dynamically learn importance scores of each modality as weights for feature fusion. To learn robust representations for both ID classification and OOD detection, it focuses on three granularities: (a) coarse-grained binary information, learned through a binary classifier trained to distinguish ID or OOD classes, (b) fine-grained information for distinguishing ID classes, captured by multiplying ID scores predicted by the binary classifier with the multimodal representations and using a cosine classifier to analyze the magnitude information, and (c) fine-grained information for distinguishing instance-level differences, achieved through contrastive learning to capture similarity relations among ID and OOD utterances.

a shallow interaction layer and fusing all modalities through a transformer-based deep interaction module. Additionally, it augments the training data from large language models to further improve performance. Dialogue act is a type of communicative intent [34] that is more coarse-grained than the specific intent classes defined in [1]. However, previous dialogue act datasets contain only the text modality [35], [36]. [37] introduces the first multimodal dialogue act dataset, derived from MELD [38] and IEMOCAP [39], adding dialogue act annotations and proposing a triplet attention subnetwork to capture intra- and inter-modality characteristics. In this work, we use MIntRec, MELD-DA, and IEMOCAP-DA as benchmark multimodal intent datasets. As the current state-of-the-art method, TCL-MAP [11] aligns non-verbal modalities with text, generates modality-aware prompts using a cross-modal transformer, and further employs contrastive learning on masking tokens aided by the generated prompts. While achieving strong performance on ID classes of MIntRec and MELD-DA, it exhibits poor generalization on unseen OOD data in our experiments.

### B. Multimodal Fusion Methods

With the emergence of multimodal language datasets in recent years [40]–[42], there has been significant interest in exploring multimodal feature fusion techniques, aiming to combine features from multiple modalities to capture their interactions. Early methods utilized tensor operations for multimodal fusion based on the rich semantics underlying high-dimensional representations [43], [44]. However, these methods struggle to balance computational cost and model performance. To address this issue, MFN [45] provides a solution by learning view-specific interactions and employing an attention mechanism with a multi-perspective gated memory.

In recent years, researchers have used transformer-based methods for multimodal fusion due to the great performance and efficiency of transformers in natural language processing and computer vision. For example, MulT [7] uses directional pairwise cross-modal attention for fusing multimodal sequences to adapt information streams from one modality to another. MAG-BERT [9] attaches a multimodal adaptation gate to transformers, allowing it to receive information from different modalities during fine-tuning. MISA [8] separates each modality into modality-invariant and modality-specific subspaces for fine-grained fusion. MMIM [46] designs a hierarchical mutual information maximization method that successively maximizes in inter-modality and fusion levels. UniMSE [47] proposes a general framework that unifies both multimodal emotion recognition and sentiment analysis tasks, formulating these tasks into a universal label format and incorporating a multimodal fusion layer into the pre-trained model T5 [48], learning inter-modality interactions with contrastive learning. However, the required label formats are not applicable to our task. In this work, we apply MulT, MAG-BERT, and MMIM as powerful multimodal fusion baselines due to their excellent performance in multimodal intent recognition.

### C. OOD Detection

Research on out-of-distribution (OOD) detection can be broadly categorized into two main aspects. On one hand, researchers have focused on learning robust representations for achieving better OOD detection performance. [17], [26] attempt to learn more robust representations of IND data. [49] utilizes unlabeled data to generate pseudo-OOD data. [50] leverages latent categorical information by training a transformer-based sentence encoder for pseudo-labeling and then performing pseudo-label learning. [51] designs a domain-regularized module to alleviate overconfidence in classifiers.

[52] proposes a two-stage method that first learns to generate synthetic ID samples for data enrichment and then adopts a training approach with  $K+1$  classes for discriminative training in OOD detection. However, these methods are constrained to the text modality and fail to leverage non-verbal modalities.

On the other hand, many works design scoring functions to calibrate model outputs for OOD detection. For example, [16] applies the energy score by calculating the logsumexp on logits. [53] uses the minimum Mahalanobis distance between features and class centroids as a confidence score. [54] focuses on the residual norm between a feature and its low-dimensional embedded pre-image. VIM [55] combines information from both features and categories, using the residual norm in [54] as a virtual logit component to calculate its softmax probability. In this work, we directly apply these scoring functions after the model outputs and compare the performance in Section V-C.

### III. THE PROPOSED APPROACH: MINTOOD

This section formulates the problem of multimodal intent classification and OOD detection and introduces a novel method, MIntOOD, as illustrated in Figure 2.

#### A. Problem Formulation

Given an intent dataset  $\mathcal{D} = \{\mathcal{D}_{\text{ID}}, \mathcal{D}_{\text{OOD}}\}$ , where  $\mathcal{D}_{\text{ID}}$  and  $\mathcal{D}_{\text{OOD}}$  denote ID and OOD data, respectively. The ID data appears in training, validation, and testing sets, while the OOD data only appears in the testing set.

**ID Classification.** Let  $\mathcal{D}_{\text{ID}} = \{(x_i, y_i) | y_i \in \mathcal{I}\}_{i=1}^{N_{\text{ID}}}$  denote the ID dataset consisting of  $N_{\text{ID}}$  instances, where  $x_i = (x_i^{\text{T}}, x_i^{\text{V}}, x_i^{\text{A}})$  represents the  $i^{\text{th}}$  utterance with text, video, and audio modalities,  $\mathcal{I} = \{\mathcal{I}\}_{i=1}^K$  is the set of intent labels, and  $K$  is the number of intent classes. The goal is to accurately predict the label  $y_i$  for each utterance  $x_i$ .

**OOD Detection.** Let  $\mathcal{D}_{\text{OOD}} = \{(x_j, y_j) | y_j = y_{\text{OOD}}, y_j \notin \mathcal{I}\}_{j=1}^{N_{\text{OOD}}}$  denote the OOD dataset containing  $N_{\text{OOD}}$  utterances that do not belong to any of the known classes. Here,  $y_{\text{OOD}}$  is a unified special token marking the labels of all OOD data. The goal is to distinguish the OOD utterances from the ID utterances in the testing set.

#### B. Feature Extraction and OOD Data Generation

**Feature Extraction.** Following [1], [42], we initially extract feature embeddings for text, video, and audio modalities to facilitate efficient multimodal fusion. For each text utterance  $x^{\text{T}}$ , we obtain the embeddings  $\mathbf{E}^{\text{T}} = \{\mathbf{E}_{[\text{CLS}]}^{\text{T}}, \mathbf{E}_1^{\text{T}}, \dots, \mathbf{E}_{[\text{SEP}]}^{\text{T}}\} \in \mathbb{R}^{L_{\text{T}} \times D_{\text{T}}}$ , by summing the corresponding token, segment, and position embeddings from the pre-trained BERT language model [24]. For each video segment  $x^{\text{V}}$ , we acquire the image sequence embeddings  $\mathbf{E}^{\text{V}} \in \mathbb{R}^{L_{\text{V}} \times D_{\text{V}}}$  using the advanced Swin Transformer vision backbone [56], as verified by its effectiveness in [11]. For the audio modality, we first process audio waveform data with the librosa toolkit [57], as adopted in [1]. Then, the state-of-the-art speech pre-trained model WavLM [58] is employed to extract audio sequence embeddings  $\mathbf{E}^{\text{A}} \in \mathbb{R}^{L_{\text{A}} \times D_{\text{A}}}$ . Here,  $L_{\text{T}}$ ,  $L_{\text{V}}$ , and  $L_{\text{A}}$  denote the sequence lengths of text, video, and audio modalities,

respectively, while  $D_{\text{T}}$ ,  $D_{\text{A}}$ , and  $D_{\text{V}}$  indicate the feature dimension of these modalities. It is important to note that all multimodal fusion methods use the same tri-modal feature embeddings as inputs to ensure a fair comparison.

**OOD Data Generation.** The process of annotating high-quality OOD data in real-world scenarios is often prohibitively costly [59]. To mitigate this, our approach leverages ID embeddings for each modality (i.e.,  $\mathbf{E}_{\text{ID}}^{\text{T}}$ ,  $\mathbf{E}_{\text{ID}}^{\text{A}}$ , and  $\mathbf{E}_{\text{ID}}^{\text{V}}$ ) to construct pseudo OOD data, thereby facilitating the differentiation between ID and OOD data in multimodal representations. Specifically, we first randomly select  $k$  embedded examples from each batch of training samples, ensuring they originate from at least two distinct classes. We then create convex combinations of these selected samples to generate the  $i^{\text{th}}$  OOD embedding:

$$\mathbf{E}_{\text{OOD},i}^{\text{M}} = \sum_{j=1}^k \lambda_j \cdot \mathbf{E}_{\text{ID},j}^{\text{M}}, \quad (1)$$

$$\text{s.t. } \lambda \sim \text{Dir}(\alpha), |\mathcal{C}(\{y_j\}_{j=1}^k)| \geq 2, \quad (2)$$

where  $\text{M} \in \{\text{T}, \text{V}, \text{A}\}$  denotes the modality. By sampling from a Dirichlet distribution  $\text{Dir}(\alpha)$ , we obtain a set of coefficients  $\{\lambda_j\}_{j=1}^k$  that satisfy  $\sum_{j=1}^k \lambda_j = 1$ , with each  $\lambda_j \in [0, 1]$ . This ensures that the convex combination represents a valid multivariate statistical mixture. Here,  $\alpha$  is a hyper-parameter that controls the diversity of the constructed OOD data. The function  $\mathcal{C}(\cdot)$  denotes the unique classes among the labels of the selected samples  $\{y_j\}_{j=1}^k$ , and  $|\cdot|$  denotes the set size.

Compared with previous manifold mixup methods for OOD generation [60], [18], which primarily rely on binary sample mixing selections, our approach introduces a novel perspective by incorporating diversity through Dirichlet distribution sampling among a batch of samples. This generates a broader range of OOD embeddings, enhancing the model's ability to generalize across various OOD scenarios. Additionally, it effectively mitigates the risk of overfitting to the ID data, fostering a more robust learning process that improves the model's performance on unseen OOD data.

#### C. Multimodal Fusion

**Multimodal Encoders.** To capture high-level semantic relationships and comprehend temporal information within text, video, and audio modalities, we employ a multi-headed attention mechanism across feature embeddings  $\mathbf{E}^{\{\text{T}, \text{V}, \text{A}\}}$  using transformer-based encoders. For the text modality, we utilize the pre-trained BERT model [61] as the encoder:

$$\mathbf{x}^{\text{T}} = \text{BERT}(\mathbf{E}^{\text{T}})_{[\text{CLS}]}, \quad (3)$$

where  $\mathbf{x}^{\text{T}} \in \mathbb{R}^{D_{\text{T}}}$ . Here, the first [CLS] token from the last hidden layer of BERT serves as the sentence-level representation, as suggested in [1]. Then, we employ vanilla transformers [62] to obtain video and audio features  $\mathbf{x}^{\text{A}}$  and  $\mathbf{x}^{\text{V}}$ :

$$\mathbf{x}^{\text{A}} = \mathbf{W}_e^{\text{A}}(\text{mean-pooling}(\text{Transformer}_{\text{A}}(\mathbf{E}^{\text{A}}))), \quad (4)$$

$$\mathbf{x}^{\text{V}} = \mathbf{W}_e^{\text{V}}(\text{mean-pooling}(\text{Transformer}_{\text{V}}(\mathbf{E}^{\text{V}}))), \quad (5)$$

where  $\mathbf{W}_e^{\text{A}} \in \mathbb{R}^{D_{\text{A}} \times D_{\text{H}}}$  and  $\mathbf{W}_e^{\text{V}} \in \mathbb{R}^{D_{\text{V}} \times D_{\text{H}}}$ . Unlike the text modality, which uses specific token embeddings, sentence-level representations for video and audio are achieved by

first applying mean pooling to the outputs of the respective transformer encoders, and then projecting them into the same dimension as the text modality for further multimodal fusion.

**Weighted Feature Fusion Network.** After encoding each modality into semantically rich representations  $\mathbf{x}^{\{T,A,V\}}$ , we explore multimodal fusion. A common approach in many traditional multimodal fusion architectures is directly performing concatenation or addition operations, as widely used in the literature [7], [8], [46]. However, we argue that each modality should be weighted differently to reflect its relative importance in the fusion process. To this end, we devise a simple yet effective weighted feature fusion network.

Given that static weights may not effectively capture the nuances of different multimodal contexts, we introduce learning dynamic weights adaptive to these contexts. Specifically, we employ three distinct neural networks, one for each modality, to compute the modality-specific importance score  $s^M \in \mathbb{R}$ :

$$s^M = \mathbf{W}_2^M(\text{Dropout}(\text{ReLU}(\mathbf{W}_1^M(\mathbf{x}^M))))), \quad (6)$$

where  $\mathbf{W}_1^M \in \mathbb{R}^{D_M \times H_w}$ , and  $\mathbf{W}_2^M \in \mathbb{R}^{H_w \times 1}$  are the weight matrices, and  $H_w$  denotes the size of the hidden layer. These non-linear layers enable each modality to learn its weighted contribution according to its contextual relevance, thereby enhancing the model’s adaptability to complicated semantics. The scores of each modality are normalized with the Softmax operation to obtain their respective weights  $w^M \in (0, 1)$ :

$$w^M = \frac{\exp(s^M)}{\sum_{M \in \{T,A,V\}} \exp(s^M)}. \quad (7)$$

Then, the weights of each modality  $w^M$  are combined with the corresponding representations  $\mathbf{x}^M$  through a weighted summation to yield the fused representation  $\mathbf{z}_F$ :

$$\mathbf{z}_F = \sum_{M \in \{T,A,V\}} w^M \cdot \mathbf{x}^M. \quad (8)$$

The proposed fusion network introduces a novel approach by dynamically learning modality weights through neural networks, which contrasts with traditional fusion strategies that rely on simple methods such as vector concatenation or addition. Unlike recent transformer-based methods, such as cross-modal attention mechanisms [7], [10] or those conditioned on semantic shifts in non-verbal modalities [9], these approaches often overlook the varying importance of different modalities or treat one modality (e.g., text) as dominant, with the others serving as secondary. This can lead to suboptimal fusion, where the contributions of each modality are not appropriately balanced. In contrast, our method enhances fusion by adaptively weighting each modality based on its contextual relevance, resulting in a more effective integration of multimodal data. As demonstrated in Section V-B, this approach significantly outperforms existing fusion techniques in terms of both flexibility and performance.

#### D. Multimodal Representation Learning

To learn robust representations for both ID classification and OOD detection, we aim to improve the discrimination ability

of each multimodal sample among ID and pseudo-OOD data at both coarse-grained and fine-grained levels.

Coarse-grained distinction primarily focuses on binary classification tasks (i.e., distinguishing between ID and OOD). This stage aims to capture more global and general characteristics of the data [63]. The model first learns to identify modality-invariant differences between ID and OOD samples, which is crucial for establishing an initial decision boundary in the multimodal feature space. This coarse distinction provides the foundation for further multimodal representation learning, where more complex interactions can be explored.

**Binary Training.** To learn basic distinguishing semantics, we employ both ID and the generated OOD data for binary classification. Specifically, we introduce the binary classifier  $\Phi_b \in \mathbb{R}^{D_H \times 2}$ , which consists of a stack of two non-linear layers. The Softmax operation is applied to the classifier outputs to obtain the prediction probabilities  $P_b = \text{Softmax}(\Phi_b(\mathbf{z}^{\text{Fusion}}))$ , serving as confidence scores. We use binary cross-entropy to define the loss in the coarse-grained training stage  $\mathcal{L}_{\text{coarse}}$ :

$$\mathcal{L}_{\text{coarse}} = -\frac{1}{B} \sum_{i=1}^B \sum_{c \in \{0,1\}} [y_{b,i}^c \log(P_{b,i}^c)], \quad (9)$$

where  $B$  is sample count in a mini-batch, and  $y_b$  denotes the binary labels with 0 indicating OOD and 1 indicating ID.

Fine-grained distinction refines the model’s discriminative ability by focusing on distinguishing more subtle differences within ID multimodal data or between instance-level ID and OOD multimodal samples. This level of discrimination goes beyond simply separating ID and OOD samples; it seeks to capture more intricate and detailed features, such as subtle variations in multimodal representations [13]. This is particularly useful for detecting pseudo-OOD samples that are highly similar to ID data in the feature space [64]. In this stage, we apply multi-class training and contrastive learning, enabling the model to capture intricate cross-modal relationships and improve its sensitivity to these subtle differences.

**Multi-class Training.** After mastering basic distinguishing characteristics, we advance to learning fine-grained discrimination information. We initially focus on capturing inter-class separation properties within ID data. Directly performing multi-class classification ignores the varying difficulties of each sample, hindering efficient training [13]. Thus, we assign confidence scores to each sample as prior knowledge and integrate them into the multimodal representations to better gauge each sample’s difficulty, thereby improving the multi-class classification training process.

To achieve this, we first obtain the binary confidence scores  $P_b^1$  as predicted by the well-trained binary classifier on the ID data. We then adjust these scores and multiply the adjusted values with the fused multimodal representations:

$$\mathbf{z}'_F = \frac{P_b^1}{1 - P_b^1} \cdot \mathbf{z}_F, \quad (10)$$

where the *odds ratio* [65] is computed as the ratio between the probability of the positive class  $P_b^1$  and the probability of the negative class (i.e.,  $1 - P_b^1$ ), which maps the output probabilities

to a more distinct, unbounded scale. Specifically, it is used to compare the probabilities between different classes to assess the likelihood of a sample being from one class rather than another. This transformation enhances the model’s sensitivity to subtle differences in probabilities by increasing the contrast between high-confidence and low-confidence predictions.

Next, we aim to utilize the transformed confidence information effectively. For this purpose, we employ the cosine classifier [66], which enables the perception of confidence information through representation magnitudes. The cosine classifier  $\Phi_{\text{cos}} \in \mathbb{R}^{D_H \times K}$  is defined as follows:

$$\Phi_{\text{cos}}(\mathbf{z}'_F) = \gamma \cdot \frac{\mathbf{z}'_F}{\|\mathbf{z}'_F\|_2} \cdot \frac{\mathbf{W}_{\text{cos}}^\top}{\|\mathbf{W}_{\text{cos}}\|_2}, \quad (11)$$

where  $K$  is the number of ID classes,  $\gamma$  is the scaling factor that controls the output logits within a proper range, and  $\|\cdot\|_2$  denotes the L2 norm. This classifier computes the cosine similarities between the representations  $\mathbf{z}'_F$  and weight matrices  $\mathbf{W}_{\text{cos}}$  by first performing L2 normalization on each and then the dot product. With the cosine classifier, samples with lower confidence scores tend to yield low classification logits with smaller magnitudes, encouraging the model to focus more on these challenging samples during training. Our experiments demonstrate that the cosine classifier generally outperforms the conventional linear layer in both ID classification and OOD detection (referred to as *w/o Cosine* in Table III).

We train the cosine classifier with the softmax loss under the supervision of multi-class labels from the ID data:

$$\mathcal{L}_m = -\frac{1}{B} \sum_{i=1}^B \sum_{c \in \mathcal{Y}} [y_{m,i}^c \log(\text{Softmax}(\Phi_{\text{cos}}(\mathbf{z}'_F))^c)], \quad (12)$$

where  $\mathcal{Y} \in \{0, 1, \dots, K-1\}$  denotes the ID label set.

**Contrastive Learning.** In addition to capturing fine-grained inter-class separation among ID data, we also explore instance-level interactions between ID and OOD data. These interactions are crucial for enhancing the model’s generalization ability across both tasks. To leverage these insights, we apply contrastive learning to both ID and the generated OOD data.

We define samples with identical labels within ID data or each sample with its augmentations as positive pairs. All other combinations are considered negative pairs. Each piece of OOD data is treated as negative when paired with other samples. This is because the pseudo-OOD samples are convex combinations of multimodal representations from various ID classes, exhibiting significant semantic differences in the feature space. The contrastive losses are defined as follows:

$$\begin{aligned} \mathcal{L}_{\text{cl-ID}} = & \\ & -\frac{1}{2N} \sum_{i \in \mathcal{N}_{\text{ID}}} \frac{1}{|\mathcal{P}(i)|} \sum_{p \in \mathcal{P}(i)} \log \frac{\exp(\text{sim}(\mathbf{l}_i, \mathbf{l}_p)/\tau)}{\sum_{k=1}^{2N} \mathbb{I}_{[k \neq i]} \exp(\text{sim}(\mathbf{l}_i, \mathbf{l}_k)/\tau)}, \end{aligned} \quad (13)$$

$$\mathcal{L}_{\text{cl-ODD}} = -\frac{1}{2N} \sum_{j \in \mathcal{N}_{\text{OOD}}} \log \frac{\exp(\text{sim}(\mathbf{l}_j, \tilde{\mathbf{l}}_j)/\tau)}{\sum_{k=1}^{2N} \mathbb{I}_{[k \neq j]} \exp(\text{sim}(\mathbf{l}_j, \mathbf{l}_k)/\tau)}, \quad (14)$$

where  $\mathcal{N}_{\text{ID}}$  and  $\mathcal{N}_{\text{OOD}}$  denote the sets of indices for ID and OOD data, respectively.  $\mathcal{P}(i)$  refers to the indices of the

samples sharing the same labels as  $i$ .  $\Phi_{\text{cl}}$  is a linear layer tailored for contrastive learning, and  $\text{sim}(\mathbf{l}_a, \mathbf{l}_b)$  measures the cosine similarity between two L2-normalized vectors.  $\mathbb{I}_{[\text{condition}]}$  is an indicator function that outputs 1 if the condition is met, otherwise 0.  $\tau$  represents the temperature hyper-parameter. Each mini-batch includes an equal number of ID and OOD samples with a total of  $N$  samples, using *dropout* [67] to generate a positive augmented samples per original, resulting in  $2N$  samples per mini-batch. The final contrastive loss,  $\mathcal{L}_{\text{cl}}$ , is defined as  $\mathcal{L}_{\text{cl}} = \mathcal{L}_{\text{cl-ID}} + \mathcal{L}_{\text{cl-ODD}}$ . Through  $\mathcal{L}_{\text{cl}}$ , we can fully learn the fine-grained relations among ID and OOD samples by pulling positive pairs and pushing negative pairs further apart, thereby enhancing the model’s discrimination ability among both ID and OOD data. Finally, we perform multi-class training and contrastive learning jointly to optimize the loss during the fine-grained training stage:  $\mathcal{L}_{\text{fine}} = \mathcal{L}_m + \mathcal{L}_{\text{cl}}$ .

This multi-granularity optimization introduces a hierarchical scheme that facilitates the learning process by progressively tackling tasks of increasing difficulty. Focusing too much on coarse-grained tasks may overlook important nuanced distinctions, while overemphasizing fine-grained tasks could lead to overfitting or inefficiency. Our multi-stage approach addresses this by first focusing on coarse-grained learning to establish a robust multimodal decision boundary between ID and OOD data. Building on this, the fine-grained objectives further refine the model’s ability to distinguish nuanced class-level and instance-level multimodal variations. This approach ensures that both coarse- and fine-grained distinctions are effectively balanced, improving adaptation to challenging multimodal samples and ensuring robustness in both ID classification and OOD detection.

## E. Inference

For ID classification, we use the outputs from the cosine classifier to predict logits and select the class with the highest probability as the predicted class. For OOD detection, we employ the Mahalanobis distance [53] as the scoring function on the fused representations to generate discriminative scores:

$$\begin{aligned} \text{Score}_{\text{Maha.}} = & \max_k \{(\mathbf{z}_F^{\text{Test}} - \boldsymbol{\mu}_k)^\top \mathbf{S}^{-1} (\mathbf{z}_F^{\text{Test}} - \boldsymbol{\mu}_k)\}, \quad (15) \\ \boldsymbol{\mu}_k = & \frac{1}{N_k} \sum_{y_i=k} \mathbf{z}_{F,i}^{\text{Train}}, \mathbf{S} = \sum_{k \in \mathcal{Y}} \sum_{y_i=k} (\mathbf{z}_{F,i}^{\text{Train}} - \boldsymbol{\mu}_k)(\mathbf{z}_{F,i}^{\text{Train}} - \boldsymbol{\mu}_k)^\top, \end{aligned} \quad (16)$$

where  $\mathbf{z}_F^{\text{Train}}$  and  $\mathbf{z}_F^{\text{Test}}$  denote the multimodal features extracted from the training and testing sets, respectively.  $\boldsymbol{\mu}_k$  represents the mean of the training samples from class  $k$ ,  $N_k$  corresponds to the number of samples in class  $k$ , and  $\mathbf{S}$  computes the covariance matrix of the training samples.

In our experiments, both our method and all baselines use this OOD detection approach to ensure a fair comparison. The Mahalanobis distance generally performs well across all datasets for OOD detection, and a detailed comparison with other state-of-the-art OOD detection methods is presented in Section V-C.

TABLE I

STATISTICS OF THE MINTREC, MELD-DA, AND IEMOCAP-DA DATASETS. #C, #VIDEO, AND #U DENOTE THE NUMBER OF INTENT CLASSES, VIDEOS, AND UTTERANCES, RESPECTIVELY. #TRAIN, #VALID, AND #TEST INDICATE THE NUMBER OF UTTERANCES IN THE TRAINING, VALIDATION, AND TESTING SETS. OOD UTTERANCES ONLY APPEAR IN THE TESTING SET. MAX. AND AVG. REPRESENT THE MAXIMUM AND AVERAGE LENGTHS, RESPECTIVELY.

Datasets	#C	#Video	#U	#Train	#Valid	#Test (ID / OOD)	Text Length (Max. / Avg.)	Video Length (Max. / Avg.)	Audio Length (Max. / Avg.)	Video Hours
MIntRec	20	43	2,674	1,334	445	445 / 450	30 / 7.04	230 / 54.37	480 / 118.03	1.47 (h)
MELD-DA	11	1039	9,988	6,561	937	1,875 / 615	70 / 7.95	250 / 72.99	530 / 152.43	8.75 (h)
IEMOCAP-DA	11	302	9,416	6,541	935	1,870 / 70	44 / 11.53	230 / 133.77	380 / 223.63	11.68 (h)

## IV. EXPERIMENTS

### A. Datasets

1) **Multimodal Intent Dataset:** The MIntRec dataset [1] provides a pioneering resource in this area, containing 2,224 multimodal utterances across various modalities (i.e., text, video, audio) with high-quality annotations spanning 20 fine-grained intent categories in real-world conversational scenarios. The original dataset serves as the ID data, and due to its lack of OOD data, we have manually constructed OOD data, which we describe in detail below.

**Construction of the OOD Data:** The motivation for constructing the OOD data stems from the fact that real-world scenarios often involve unexpected out-of-scope utterances that fall outside the well-annotated known classes during dialogue interactions. Such data, if not properly handled, can degrade the performance of dialogue systems. To address this challenge and mitigate the issue of data scarcity, we construct the OOD dataset through the following two key steps:

**Data Preparation:** As recommended in [1], we begin by collecting raw video clips from the TV series Superstore, ensuring that the segments we select are distinct from those included in the original dataset. These segments are chosen to reflect a variety of conversational contexts, such as different settings, characters, and emotional tones. This diversity helps ensure that the OOD data captures a broad range of potential out-of-scope scenarios. The raw video clips are then split into shorter video clips based on timestamps and subtitles. For each clip, we extract the corresponding audio segments, which are then paired with the corresponding subtitles to form multimodal data.

**Data Annotation:** We employ five annotators, each trained to carefully review the multimodal content of each sample. Before starting the annotation process, the annotators familiarize themselves with the definitions of each of the 20 intent categories and review a series of typical examples. Each annotator then labels whether a sample is an ID or OOD sample based on the textual, audio, and video information. To ensure the reliability and consistency of the annotation, we select only those samples where all five annotators agree on the classification (i.e., all five annotators label the sample as OOD). This process ensures high-quality, consistent OOD annotations. In total, 450 utterances are selected to comprise the OOD data for the MIntRec dataset.

2) **Multimodal Dialogue Act Datasets:** As dialogue acts are considered coarse-grained communicative intents during conversational interactions, we utilize two multimodal dialogue datasets, MELD-DA and IEMOCAP-DA. MELD-DA, derived from the MELD dataset [38], originates from the

TV series *Friends* and contains over 13,000 utterances from 1,433 dialogues. IEMOCAP-DA is based on the IEMOCAP dataset [39], which includes videos from both scripted plays and spontaneous interactions involving 10 actors, totaling nearly 12 hours. For dialogue act labels, we adopt the well-annotated labels from the EMOTyDA dataset [37]. The employed dialogue act taxonomies include 12 frequently appearing tags derived from the Switchboard corpus [68], encompassing 11 known classes, including *Acknowledge* (a), *Agreement* (ag), *Answer* (ans), *Apology* (ap), *Backchannel* (b), *Command* (c), *Disagreement* (dag), *Greeting* (g), *Statement-Opinion* (o), *Question* (q), and *Statement-Non-Opinion* (s), and one *Others* (oth) class, which includes all other potential dialogue act types. Therefore, we use samples within the known classes as ID data and those within the *Others* tag as OOD data. Following [69], [70], OOD data only appear in the testing set when performing OOD detection. Detailed statistics and data splits are provided in Table I.

### B. Baselines

Due to the absence of multimodal methods specifically designed for out-of-distribution (OOD) detection, we establish baselines using state-of-the-art multimodal fusion methods. These include TEXT, MuT [7], MAG-BERT [9], MMIM [46], SDIF [10], SPECTRA [71], TCL-MAP [11], as well as MIntOOD (R) and MIntOOD (T), two variants of our method. Detailed descriptions of these methods are provided below:

**TEXT:** This baseline utilizes the text-only modality. We fine-tune the pre-trained BERT language model with a classifier for intent classification, supervised by the training targets.

**MuT:** It first employs six cross-modal transformers to capture interactions between pairs of modalities. Then, for each pair of cross-modal transformers including the target modality, a self-attention mechanism is applied to the concatenated outputs with a transformer to capture temporal information.

**MAG-BERT:** It introduces a plug-and-play module that accommodates non-verbal inputs between layers of pre-trained transformers. This module calculates the displacement of non-verbal vectors and performs a weighted summation with verbal displacement vectors to produce a multimodal representation.

**MMIM:** It learns modality-invariant information by optimizing mutual information bounds between text and other modalities. It computes inverse correlations between multimodal and unimodal features, optimizing via noise contrastive estimation [72]. Entropy estimators are not used as they adhere to sentiment polarities, which are not applicable in our task.

**SPECTRA:** It consists of a text encoder, audio encoder, and fusion module, pre-trained on a temporal position prediction

task for explicit text-audio alignment, and fine-tuned for enhanced multimodal intent recognition.

**TCL-MAP:** It first generates a modality-aware prompt to refine the text modality and then uses the ground truth label to create an augmented sample. Next, a contrastive learning mechanism is applied to the token to learn from the ground-truth semantics and guide the learning of nonverbal modalities.

**SDIF:** It employs a text-centric shallow interaction module to align video and audio features with text, followed by a transformer-based deep interaction module to refine cross-modal fusion.

**MIntOOD (R):** A variant of MIntOOD using real OOD data for training and validation. For a fair comparison, the OOD data from the MELD-DA dataset is used for the MIntRec dataset, while the OOD data from the MIntRec dataset is used for the MELD-DA and IEMOCAP-DA datasets.

**MIntOOD (T):** A variant of MIntOOD, the main difference being its use of sentence-level representations from BERT rather than multimodal fused representations.

### C. Evaluation Metrics

**ID Classification:** To evaluate the performance of ID classification, we use six metrics: accuracy (ACC), weighted F1-score (WF1), weighted precision (WP), F1-score (F1), precision (P), and recall (R). These metrics are defined as follows:

$$P = \frac{1}{K} \sum_{i=1}^K \frac{TP_{C_i}}{TP_{C_i} + FP_{C_i}}, R = \frac{1}{K} \sum_{i=1}^K \frac{TP_{C_i}}{TP_{C_i} + FN_{C_i}}, \quad (17)$$

$$ACC = \sum_{i=1}^T \mathbb{I}(y^{\text{Pred}} = y^{\text{GT}}), F1 = 2 \times \frac{P \times R}{P + R}, \quad (18)$$

$$WP = \frac{1}{K} \sum_{i=1}^K \frac{T_{C_i}}{T} \times \frac{TP_{C_i}}{TP_{C_i} + FP_{C_i}}, \quad (19)$$

$$WF1 = \frac{1}{K} \sum_{i=1}^K \frac{T_{C_i}}{T} \times \frac{2 \times P_{C_i} \times R_{C_i}}{P_{C_i} + R_{C_i}}, \quad (20)$$

where  $K$  is the number of classes,  $C_i$  is the  $i^{\text{th}}$  class, and TP, FP, FN denote the true positives, false positives, and false negatives, respectively.  $y^{\text{Pred}}$  denotes the predicted labels,  $y^{\text{GT}}$  the ground truth labels,  $T$  the total number of ID samples in the testing set, and  $T_{C_i}$  the number of ID samples from class  $C_i$  in the testing set.

**OOD Detection:** Following [53], [70], [73], we evaluate OOD detection performance using five typical metrics: DER, FPR95, AUPR-In, AUPR-Out, and AUROC. These metrics were selected to comprehensively assess OOD detection performance under different conditions. Lower values are preferable for the first two metrics, while higher values are preferable for the latter three. The details of these metrics are as follows:

(1) **FPR95:** Defined as the false positive rate when the true positive rate (TPR) is at least 95%, it represents the probability of an OOD sample being misclassified as ID. Here, TPR is defined as:  $TP / (TP + FN)$ . (2) **DER:** Calculated as  $P_{\text{ID}} \cdot (1 - \text{TPR}) + P_{\text{OOD}} \cdot \text{FPR}$  when TPR is 95%. We assume an equal appearance probability of ID and OOD

samples during testing, as suggested in [70]. Here, FPR is defined as:  $FP / (TN + FP)$ , where TN denotes the number of true negatives. (3) **AUPR:** The area under the precision-recall curve, with AUPR-In and AUPR-Out treating ID and OOD samples as positives, respectively. (4) **AUROC:** The area under the receiver operating characteristic curve, illustrating the relationship between TPR and FPR at various thresholds. These five metrics together offer a robust evaluation of the model’s OOD detection capabilities across various thresholds, balancing the trade-off between rejecting OOD samples and correctly classifying ID samples.

### D. Experimental Settings

In the experiments, ID data presents in the training, validation, and testing sets, while OOD data only appears in the testing set. Each method is tuned using the ID data from the validation set with the best model saved using an early stopping strategy. During inference, we evaluate the ID classification performance using the ID data and generate Mahalanobis scores as defined in Eq. 16 for both ID and OOD data to assess OOD detection performance.

For feature extraction, sequence lengths  $L_T$ ,  $L_V$ , and  $L_A$  are set to (30, 230, 480), (70, 250, 530), and (44, 230, 380) for the MIntRec, MELD-DA, and IEMOCAP-DA datasets, respectively. Feature dimensions  $D_T$ ,  $D_V$ , and  $D_A$  are set to 768, 1024, and 768, respectively. During OOD data generation, the number of selected embedded examples  $k$  is set to 3 for all three datasets. The sampling parameter  $\alpha$  of the Dirichlet distribution is set to (2, 0.7, 0.7). The hidden feature dimension  $D_H$  is set to 768, and the hidden size of the weighted feature fusion network  $H_w$  is 256. The scaling factor  $\gamma$  in the cosine classifier is set to (16, 16, 32), and the temperature  $\delta$  for contrastive learning is set to (2, 1, 0.7). The number of training epochs is 100, and the batch size is 32. We utilize the PyTorch library implemented in HuggingFace [74] for the pre-trained BERT language model, adopting the AdamW [75] optimizer with learning rates of (3e-5, 4e-6, 3e-6). For a fair comparison, all experimental results are reported as averages from five runs with random seeds ranging from 0 to 4. The experiments are conducted on an NVIDIA Tesla V100-SXM2.

## V. RESULTS AND DISCUSSION

### A. Main Results

The main experimental results of ID classification and OOD detection are presented in Table II. Within each evaluation metric, the best performance is highlighted in bold and the second-best result is underscored. MIntOOD achieves superior performance across all three datasets, especially showing significant improvements in OOD detection performance, which demonstrates the efficacy and robustness of the learned multimodal representations in these tasks.

For ID classification, compared to the best-performing baselines, our method consistently outperforms the baselines by over 1-2% on all metrics except recall on the MIntRec dataset. It also achieves improvements of more than 0.5% on half of the evaluation metrics on the MELD-DA dataset and over 5% on the precision metric. While SPECTRA stands out in the

TABLE II  
ID CLASSIFICATION AND OOD DETECTION RESULTS ON THE MINTREC, MELD-DA, AND IEMOCAP-DA DATASETS.

Datasets	Methods	ID Classification						OOD Detection				
		ACC ( $\uparrow$ )	WF1 ( $\uparrow$ )	WP ( $\uparrow$ )	F1 ( $\uparrow$ )	P ( $\uparrow$ )	R ( $\uparrow$ )	DER ( $\downarrow$ )	FPR95 ( $\downarrow$ )	AUPR In ( $\uparrow$ )	AUPR Out ( $\uparrow$ )	AUROC ( $\uparrow$ )
MIntRec	TEXT	70.34	70.46	71.12	67.06	67.53	67.24	40.25	76.00	74.52	75.14	76.23
	MAG-BERT	72.00	71.78	72.45	68.36	69.01	68.92	41.80	79.07	74.05	71.31	74.48
	MuIT	72.31	72.07	72.24	68.97	69.73	68.83	42.13	79.78	74.77	71.45	75.21
	MMIM	72.05	71.97	72.80	69.68	70.59	69.81	40.45	76.45	75.84	73.89	75.85
	SPECTRA	71.01	70.83	71.90	67.87	69.41	68.10	40.78	77.02	74.88	73.92	75.35
	TCL-MAP	73.21	72.73	73.02	69.02	69.39	69.88	41.40	78.31	74.71	73.19	75.36
	SDIF	71.42	71.24	71.82	68.53	70.33	67.86	39.77	75.42	72.47	73.06	73.40
	MIntOOD (R)	72.18	71.86	72.59	68.29	69.75	68.43	40.08	75.60	77.67	75.35	78.55
	MIntOOD (T)	72.14	71.78	72.00	68.30	68.88	68.45	37.44	70.31	76.57	78.38	78.95
	MIntOOD	<b>74.34</b>	<b>74.15</b>	<b>74.51</b>	<b>70.94</b>	<b>72.24</b>	<b>70.46</b>	<b>36.03</b>	<b>67.56</b>	<b>79.69</b>	<b>80.09</b>	<b>80.54</b>
MELD-DA	TEXT	63.54	62.59	62.64	54.48	57.07	53.55	59.67	77.63	84.57	44.55	67.38
	MAG-BERT	64.50	63.16	63.14	54.30	58.81	53.51	58.07	75.54	86.63	49.02	72.32
	MuIT	63.35	62.28	62.96	54.20	58.45	53.57	63.03	82.08	86.25	40.82	69.62
	MMIM	64.45	63.08	63.57	55.27	59.88	54.02	56.03	72.78	87.74	51.59	73.83
	SPECTRA	60.81	60.31	60.93	54.62	55.66	55.28	63.57	82.83	83.68	40.36	64.62
	TCL-MAP	64.23	62.94	62.73	53.98	57.10	53.22	58.48	76.03	86.17	48.82	71.79
	SDIF	64.33	63.19	63.75	55.56	62.11	54.00	56.81	73.82	87.87	49.73	74.46
	MIntOOD (R)	64.50	62.45	62.80	53.65	59.90	52.34	57.36	75.60	87.47	51.08	74.57
	MIntOOD (T)	64.32	62.61	63.58	55.16	64.71	53.33	57.26	74.37	86.88	50.49	73.40
	MIntOOD	<b>65.00</b>	<b>63.53</b>	<b>64.62</b>	<b>56.20</b>	<b>65.09</b>	<b>54.20</b>	<b>55.54</b>	<b>72.13</b>	<b>88.85</b>	<b>54.45</b>	<b>76.95</b>
IEMOCAP-DA	TEXT	73.97	73.88	74.53	70.28	70.18	72.00	57.67	59.71	99.45	22.54	87.92
	MAG-BERT	74.52	74.33	74.64	70.80	71.70	71.59	87.38	90.57	99.30	14.03	84.30
	MuIT	73.87	73.73	73.97	70.75	72.01	70.25	90.68	94.00	99.04	7.97	77.69
	MMIM	74.48	74.32	74.69	71.92	73.08	71.83	71.18	73.72	99.09	15.45	79.94
	SPECTRA	74.54	74.43	74.93	70.35	72.17	70.10	93.42	96.86	99.23	10.20	81.47
	TCL-MAP	74.61	74.44	74.72	72.15	74.37	70.98	95.87	99.43	98.77	6.61	71.72
	SDIF	74.49	74.38	74.81	72.18	74.64	70.89	64.33	66.57	99.55	18.94	88.83
	MIntOOD (R)	74.47	71.86	72.59	68.29	69.75	68.43	14.19	14.57	99.85	85.08	96.52
	MIntOOD (T)	74.46	74.36	74.73	71.50	73.19	70.75	29.87	30.86	99.76	40.13	94.63
	MIntOOD	<b>74.88</b>	<b>74.77</b>	<b>75.24</b>	<b>72.82</b>	<b>74.28</b>	<b>72.42</b>	<b>12.82</b>	<b>13.14</b>	<b>99.88</b>	<b>84.03</b>	<b>97.19</b>

TABLE III  
ABLATION STUDIES ON THE MINTREC, MELD-DA, AND IEMOCAP-DA DATASETS.

Datasets	Methods	ID Classification						OOD Detection				
		ACC ( $\uparrow$ )	WF1 ( $\uparrow$ )	WP ( $\uparrow$ )	F1 ( $\uparrow$ )	P ( $\uparrow$ )	R ( $\uparrow$ )	DER ( $\downarrow$ )	FPR95 ( $\downarrow$ )	AUPR In ( $\uparrow$ )	AUPR Out ( $\uparrow$ )	AUROC ( $\uparrow$ )
MIntRec	Fusion (Add)	73.04	72.71	73.21	68.64	70.09	68.43	38.39	72.45	77.84	78.43	78.78
	Fusion (Concat)	72.90	72.67	72.95	68.91	69.94	68.66	38.90	73.29	78.07	77.57	79.06
	Fusion (MuIT)	71.19	70.75	71.75	67.64	69.34	67.82	40.85	77.16	76.11	74.15	76.46
	Fusion (MAG-BERT)	72.27	71.92	72.87	68.44	69.36	69.14	39.12	73.78	76.41	76.17	78.12
	Fusion (SDIF)	71.82	71.47	71.67	68.70	70.03	68.19	39.45	74.36	77.12	76.46	77.64
	w / o Contrast	72.90	72.74	73.32	69.38	70.69	69.12	37.93	71.42	78.84	78.90	79.83
	w / o Cosine	68.90	68.19	70.34	64.25	67.12	65.07	39.70	75.02	72.84	75.08	75.39
	w / o Binary	73.08	72.89	73.40	69.42	70.95	68.94	39.57	74.71	78.34	77.06	78.44
	Full	<b>74.34</b>	<b>74.15</b>	<b>74.51</b>	<b>70.94</b>	<b>72.24</b>	<b>70.46</b>	<b>36.03</b>	<b>67.56</b>	<b>79.69</b>	<b>80.09</b>	<b>80.54</b>
	MELD-DA	Fusion (Add)	63.22	61.01	61.90	52.36	58.06	50.80	56.92	73.98	88.31	51.42
Fusion (Concat)		63.65	61.34	62.63	52.75	61.50	51.19	59.85	77.89	87.19	48.11	73.17
Fusion (MuIT)		63.61	61.25	62.64	51.83	61.72	50.43	59.48	77.37	87.49	45.18	73.43
Fusion (MAG-BERT)		64.44	62.01	62.62	53.01	58.42	52.18	55.66	72.29	87.59	50.90	74.08
Fusion (SDIF)		63.47	62.23	62.62	54.56	59.16	53.16	59.10	76.88	86.27	47.16	71.37
w / o Contrast		64.13	62.12	63.01	53.95	61.87	52.45	56.95	74.02	86.67	50.25	73.27
w / o Cosine		63.00	60.58	62.24	53.63	59.22	53.21	61.83	80.49	86.47	46.54	72.47
w / o Binary		63.50	60.51	62.01	51.18	59.24	49.94	58.76	76.42	87.61	49.97	74.32
Full		<b>65.00</b>	<b>63.53</b>	<b>64.62</b>	<b>56.20</b>	<b>65.09</b>	<b>54.20</b>	<b>55.54</b>	<b>72.13</b>	<b>88.85</b>	<b>54.45</b>	<b>76.95</b>
IEMOCAP-DA		Fusion (Add)	74.57	74.44	74.83	71.14	72.21	70.99	21.92	22.57	99.81	38.75
	Fusion (Concat)	74.03	73.90	74.08	70.16	72.28	69.52	43.13	44.57	99.34	26.82	87.72
	Fusion (MuIT)	74.39	74.20	74.47	72.20	73.01	72.32	95.41	98.86	99.18	9.17	80.67
	Fusion (MAG-BERT)	74.16	74.02	74.36	71.52	72.78	71.12	64.82	67.14	99.18	30.82	82.54
	Fusion (SDIF)	74.78	74.69	75.13	71.06	73.24	70.59	75.29	78.00	99.44	22.20	86.42
	w / o Contrast	74.29	74.66	74.88	72.52	72.89	72.91	15.26	15.71	99.86	82.82	96.83
	w / o Cosine	73.11	72.88	73.24	68.76	70.30	68.71	12.80	13.14	99.88	83.14	97.29
	w / o Binary	73.93	73.75	73.92	71.07	72.31	70.98	13.92	14.29	99.86	78.06	96.83
	Full	<b>74.87</b>	<b>74.77</b>	<b>75.24</b>	<b>72.82</b>	<b>74.28</b>	<b>72.42</b>	<b>12.82</b>	<b>13.14</b>	<b>99.88</b>	<b>84.03</b>	<b>97.19</b>

recall metric on MELD-DA, our method outshines it on the remaining five metrics with a significant margin of 1–9%. On the IEMOCAP-DA dataset, our method secures state-of-the-art performance across five metrics, with only the precision metric led by SDIF. It is evident that our method shows significantly greater improvements on the MIntRec dataset than on the other datasets. This is likely because the intent categories defined in the MIntRec dataset contain more fine-grained and nuanced semantics, which are more challenging than the coarse-grained communicative intents, showcasing the advantage of our method in learning discriminative multimodal representations for intent classification. Moreover, two variants of our method, MIntOOD (R) and MIntOOD (T), display

strong and comparable performance on many metrics across the three datasets compared to the baselines. However, it underperforms relative to MIntOOD, showing a decrease of over 2% on the MIntRec dataset, underscoring the importance of non-verbal modalities in capturing complex intent semantics.

For OOD detection, our method demonstrates substantially greater improvements across all three datasets. In particular, on the MIntRec dataset, our method shows improvements of 3–9% across all evaluation metrics when compared with the best-performing baselines. On the MELD-DA dataset, MMIM and SDIF are two strong baselines that exhibits comparable performance to our method on all metrics. Nonetheless, our method still achieves more than 2% of improvement on AUPR

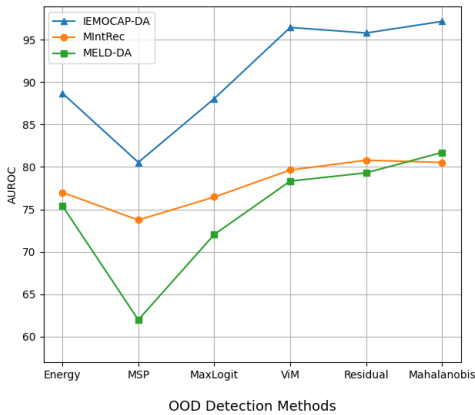


Fig. 3. A comparison between different OOD detection methods.

Out and AUROC. On the IEMOCAP-DA dataset, our method shows absolute advantages in DER, FPR95, AUPR Out, and AUROC, with improvements of 44.85%, 46.57%, 61.49%, and 8.36%, respectively. The remaining metric, AUPR In, achieves nearly 100%. This suggests that there are fewer OOD samples in the IEMOCAP-DA test set compared to others, and existing baselines tend to overfit on the ID data yet still generate high scores on OOD data, resulting in significantly poorer performance. This further demonstrates the robustness and strong generalization ability of our method when faced with unseen OOD data. MIntOOD (R) achieves outstanding results across most metrics on all three datasets, clearly surpassing the baselines. However, our method maintains a decisive advantage, outperforming MIntOOD (R) by 2–8%, 1–3%, and 0.5–1% on the respective datasets. These findings underscore the effectiveness of our OOD data generation strategy, which enhances the model’s OOD detection capability even beyond that attained with real-world OOD samples. Compared to MIntOOD (T), our method shows substantial improvements in almost all metrics in the three datasets, with about 1–3%, 2–4%, and 2–40% score improvements, showing that non-verbal modalities can yield greater gains in detecting OOD samples.

### B. Ablation Studies

To validate the effectiveness of each component in MIntOOD, we conduct ablation studies, with results shown in Table III. First, we evaluate the weighted feature fusion network by comparing it to two standard multimodal fusion method: Fusion (Add) and Fusion (Concat), and three fusion mechanisms from baselines: Fusion (MulT), Fusion (MAG-BERT) and Fusion (SDIF). Fusion (Add) adds the features of all three modalities, while Fusion (Concat) concatenates the features and projects them into the same dimension  $D_H$  using a linear layer. Fusion (MulT), Fusion (MAG-BERT), and Fusion (SDIF) use fusion networks from their respective baselines. Our method consistently outperforms the two standard fusion methods by 1–5% across most metrics for ID classification and OOD detection on the MIntRec and MELD-DA datasets. It also shows a significant improvement of up to 6.22%

over the best baseline fusion mechanism, particularly on the FPR95 metric of the MIntRec dataset. On the IEMOCAP-DA dataset, while showing marginal improvement in some ID classification metrics, our method achieves substantial gains of 9.1%, 9.43%, and 45.28% on DER, FPR95, and AUPR Out for OOD detection, respectively. These results demonstrate that the learned modality weights enhance multimodal fusion, leading to better representations compared to other strategies.

Second, we evaluate the impact of removing contrastive loss (w/o Contrast). Apart from ID classification on the IEMOCAP-DA dataset, our method shows more than 1% improvement across most metrics on both tasks across all three datasets. This suggests that fine-grained learning of ID and OOD data interactions fosters discriminative representation learning. However, its absence results in less significant decreases compared to other ablation studies, indicating its auxiliary role in enhancing multimodal representation learning. Third, we replace the cosine classifier with a linear classifier (w/o Cosine), leading to significant decreases of 2–6% in ID classification performance across the three datasets and 2–8% reductions on the MIntRec and MELD-DA datasets. This reveals that the cosine classifier is crucial for effectively discriminating features and capturing confidence information in multimodal representations. Notably, in OOD detection on IEMOCAP-DA, performance is comparable or even improves. This is likely because the OOD data in IEMOCAP-DA contains distinct features (e.g., absence of text modality) that can be recognized by a simple linear layer without normalization.

Finally, we assess the impact of removing the binary training process and binary information from the representations (w/o Binary). This leads to a decrease of over 1% in ID classification scores across all three datasets, with a particularly notable reduction of 4–6% in F1-score, precision, and recall on the MELD-DA dataset. This component also plays a significant role in OOD detection, with a 1–7% and 1–4% decrease in all OOD metrics on the MELD-DA and MIntRec datasets, respectively. These significant reductions underscore the importance of distinguishing elementary binary information and the need to leverage it to guide representation learning.

### C. Effect of OOD Detection Methods

To investigate the effect of different OOD detection methods, we compare our method, Mahalanobis (as introduced in Section III-E), with five other state-of-the-art unsupervised OOD detection methods: (1) **textbfEnergy**: This method applies the energy function [16] to the output logits. (2) **Residual**: As suggested in [55], [76], we first offset the feature space to the origin and calculate the principal subspace using the largest eigenvalues (equal to the number of ID classes) of the covariance matrix. We then measure the deviation of the features extracted from the testing set from the principal subspace by calculating the length of the features in the orthogonal complement of the principal subspace. (3) **MSP**: This method calculates the maximum Softmax probabilities [69] by applying Softmax to the neural network output logits. (4) **MaxLogit**: It involves direct maximization over the neural network output logits. (5) **ViM**: Virtual-logit matching [55]

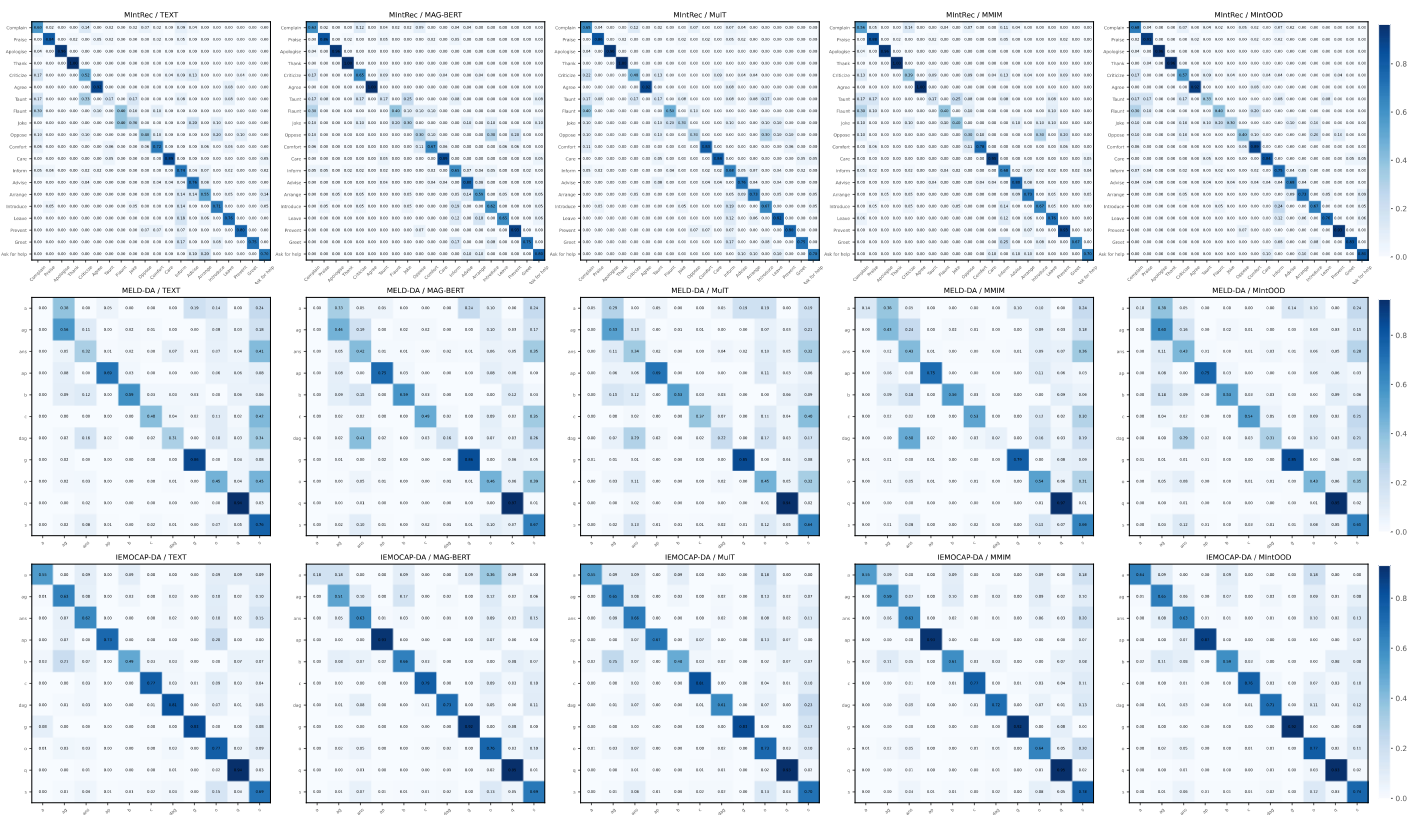


Fig. 4. Confusion matrices compare ID classes of baselines and our method across the three datasets.

adjusts the residual score to generate a virtual logit using a scaling parameter, which is derived from the ratio of the mean of the maximum training logits to the mean of the training residual scores. We then compute the ViM score by replacing the target logit of the original testing logits with the virtual logit. Before calculating the Residual and ViM scores, L2-normalization is performed on the classifier weights and features, given our method’s use of a cosine classifier.

We use AUROC as the metric and present the results in Figure 3. Mahalanobis achieves the best performance on the IEMOCAP-DA and MELD-DA datasets and the second-best performance on the MIntRec dataset, slightly lower than that of Residual, demonstrating the effectiveness of using the Mahalanobis distance in the feature space to generate discriminative scores for OOD detection. It is observed that Energy, MSP, and MaxLogit consistently show lower performance than the others. This is because they rely on the output logits from the cosine classifier, which tend to overfit on ID classes rather than capturing the discrepancy between ID and OOD, thereby limiting their generalization ability on unseen OOD data. In contrast, ViM, Residual, and Mahalanobis use more original features before the cosine classifier, incorporating broader and more fundamental characteristics that might be missed or ignored after classification. Although Residual and ViM also focus on OOD detection within the feature space, they exhibit poorer performance than Mahalanobis. This is because Residual considers only the principal subspace, neglecting other dimensions that might also play a substantial role in yielding discriminative scores. Besides, ViM incorporates information

from the output logit space, which could negatively impact the purity of the information from the feature space.

#### D. Analysis of ID Classification Performance

To investigate the fine-grained performance of ID classification, we compare our method with four baselines using confusion matrices, as shown in Figure 4. Each score on the principal diagonal indicates the accuracy score for each class.

On the MIntRec dataset, our method achieves the best performance in 12 out of 20 classes, significantly outperforming the baselines. In contrast, the baselines TEXT, MuIT, MAG-BERT, and MMIM achieve the best performance in only 4, 5, 6, and 7 classes, respectively. Specifically, our method shows improvements of 1%, 2%, 3%, 6%, 8%, and 16% over the best-performing baselines in the *Inform*, *Praise*, *Complain*, *Comfort*, *Greet*, and *Taunt* classes, respectively. It also leads in the *Apologise*, *Oppose*, *Arrange*, *Ask for help*, and *Prevent* classes. These results demonstrate that our method can effectively capture the nuanced features of ID classes, excelling in recognizing intent classes with both straightforward (e.g., *Greet*, *Praise*, *Apologise*) and complex semantics (e.g., *Complain*, *Taunt*, *Ask for help*). Our method performs comparably to the baselines in most of the remaining classes (e.g., *Thank*, *Care*, *Flaunt*, *Joke*, and *Leave*). The limited differentiation in classes such as *Thank* and *Care* is primarily because they heavily rely on textual modality, which does not significantly benefit from non-verbal modalities. Moreover, classes with intricate semantics, such as *Flaunt*, *Joke*, and

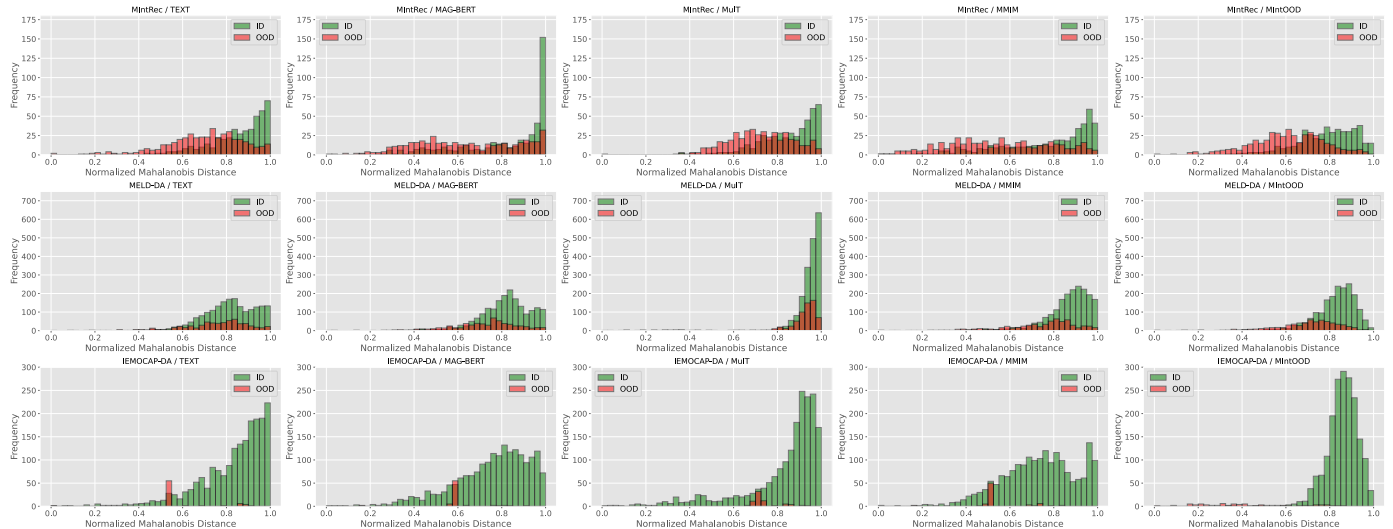


Fig. 5. Distribution of OOD detection scores for ID and OOD data in the testing sets of the three datasets.

Leave, pose challenges in capturing high-level video or audio cues like expressions, body language, and tones, which are essential for understanding the intents.

On the MELD-DA and IEMOCAP-DA datasets, our method achieves the best performance in 5 out of 11 ID classes and 4 out of 11 ID classes, respectively, maintaining its lead in the majority of categories. Specifically, on the MELD-DA dataset, MIntOOD excels in the *Agreement* (ag), *Answer* (ans), *Apology* (ap), and *Command* (c) classes, with performance improvements ranging from 1% to 4% over the best-performing baselines. Additionally, it displays comparable performance to the top baselines in the *Disagreement* (dag), *Greeting* (g), and *Question* (q) classes, with differences within 2%. On the IEMOCAP-DA dataset, MIntOOD leads in the *Acknowledge* (a), *Agreement* (ag), *Greeting* (g), and *Statement-Opinion* (o) classes. It also shows competitive performance in the *Answer* (ans), *Question* (q), and *Statement-Non-Opinion* (s) classes. Notably, it significantly enhances the *Acknowledge* class by 9%, addressing the challenges posed by the lack of textual information in responses predominantly featuring short forms. In these cases, our method effectively leverages non-verbal modalities to boost intent recognition. These results demonstrate that our proposed method excels in distinguishing ambiguous and coarse-grained communicative intents by leveraging multimodal information. While it performs well in categories with easily recognizable linguistic features, such as *Apology*, *Greeting*, and *Question*, there are still challenges in identifying abstract dialogue acts. Particularly in classes like *Acknowledge*, *Backchannel*, and *Answer*, where performances often fall below 60%, the method struggles with classes that have similar semantics. This indicates that existing multimodal fusion methods still face difficulties in learning discriminative representations for these complex semantics.

### E. Analysis of OOD Detection Performance

To illustrate the model’s capability to detect OOD data, we compute the confidence scores for each testing sample by

normalizing the Mahalanobis distance scores  $x_{Ma}$  within the range  $[0, 1]$  using min-max scaling:  $x'_{Ma} = \frac{x_{Ma} - \min(x_{Ma})}{\max(x_{Ma}) - \min(x_{Ma})}$ . We plot the distribution of scores  $x'_{Ma}$  for both ID and OOD data across three datasets, as shown in Figure 5.

On the MIntRec dataset, it is observed that MIntOOD controls the confidence scores of OOD samples to predominantly fall within the range  $[0.5, 0.7]$ , maintaining a clear separation from the majority of ID sample scores, which range  $[0.7, 0.9]$ . This delineation indicates a distinct boundary between ID and OOD samples. In contrast, the baselines exhibit more overlap between ID and OOD samples. For instance, overlaps in ID and OOD confidence scores occur within the ranges  $[0.7, 1.0]$ ,  $[0.75, 1.0]$ ,  $[0.7, 0.9]$ , and  $[0.5, 0.9]$  for TEXT, MAG-BERT, MuT, and MMIM, respectively. Consequently, MIntOOD demonstrates superior generalization capabilities on unseen OOD data with more discriminative representations.

On the MELD-DA dataset, all baselines fail to effectively distinguish between ID and OOD samples. Specifically, the distances between ID and OOD distribution peaks are approximately 0, 0.075, 0.025, and 0.1 for TEXT, MAG-BERT, MuT, and MMIM, respectively. In contrast, MIntOOD shows a much greater separation, with a distance of 0.175, clearly indicating fewer overlaps between OOD and ID samples compared to the baselines. However, there remains a certain degree of overlap in all methods. This overlap is partly due to the *Others* class used as OOD data having similar linguistic characteristics to ID data, which include ambiguous semantics that are difficult to differentiate, thus posing challenges for OOD detection.

On the IEMOCAP-DA dataset, MIntOOD exhibits exceptional performance, nearly completely distinguishing ID from OOD data with minimal overlap. In comparison, other methods show a significant amount of overlap, with over 50% of OOD data overlapping with ID data. Despite the sparse presence of OOD data in the IEMOCAP-DA dataset, our method avoids overfitting to ID data and demonstrates remarkable robustness and discrimination capabilities, with most OOD scores below 0.5 and the majority of ID scores above 0.6. These results

underscore the effectiveness of MIntOOD, which leverages specifically designed multimodal fusion and discriminative representation learning techniques to demonstrate strong generalization capabilities and reliability in detecting OOD data.

## VI. CONCLUSIONS

This paper proposes MIntOOD, a novel method designed to address the critical challenge of multimodal intent understanding by both accurately recognizing known intents and effectively detecting unseen OOD data. MIntOOD comprises two main modules. First, it introduces a simple yet effective multimodal fusion network that learns the weights of each modality through respective learnable neural networks. These learned weights are combined with the original encoded modality-specific features to produce multimodal representations. This strategy outperforms traditional concatenation or addition fusion strategies, particularly in OOD detection performance. Second, we explore the development of friendly representations conducive to both tasks from three perspectives. After generating pseudo-OOD data from ID data, we initially learn coarse-grained features by distinguishing between the binary classes of ID and OOD. Subsequently, we refine our approach by using binary scores as confidence indicators to guide the learning of challenging samples to distinguish between different ID classes. We also utilize instance-level similarity relations to further enhance discriminative representation learning. Each of these strategies plays a crucial role, and their removal would result in a substantial decrease in performance, underscoring their effectiveness.

We establish baselines on three typical benchmark multimodal intent datasets. An OOD benchmark is specifically built for the MIntRec dataset due to its previous absence. Extensive experiments demonstrate that our proposed method consistently achieves the best performance on ID classification across the three datasets. Moreover, it significantly outperforms the baselines in OOD detection, with increases of up to 3-62% on the AUPR Out metric. Further analysis on ID classification and OOD detection provides additional evidence of the robustness and effectiveness of our method. We believe this work represents a significant advancement and serves as a pioneering success in this field.

## REFERENCES

- [1] H. Zhang, H. Xu, X. Wang, Q. Zhou, S. Zhao, and J. Teng, "Mintrec: A new dataset for multimodal intent recognition," in *Proc. of the 30th ACM Int. Conf. on Multimedia*, 2022, pp. 1688–1697.
- [2] K. Wang, S. Lian, H. Sang, W. Liu, Z. Liu, F. Shi, H. Deng, Z. Sun, and Z. Chen, "Multimodal activity detection for natural interaction with virtual human," *2023 IEEE Conf. Virtual Reality 3D User Interfaces Abstr. Workshops*, pp. 671–672, 2023.
- [3] Y. Fan, C. Wang, P. He, and Y. Hu, "Building multi-turn query interpreters for e-commercial chatbots with sparse-to-dense attentive modeling," in *Proc. 15th ACM Int. Conf. Web Search Data Mining*, 2022, p. 1577–1580.
- [4] S. Paul, M. Sintek, V. Kępuska, M. Silaghi, and L. Robertson, "Intent based multimodal speech and gesture fusion for human-robot communication in assembly situation," in *2022 21st IEEE Int. Conf. Mach. Learn. Appl.*, 2022, pp. 760–763.
- [5] Z. Zhang, "Towards a multimodal and context-aware framework for human navigational intent inference," *Proc. 2020 Int. Conf. Multimodal Interaction*, 2020.
- [6] J. Mi, S. Tang, Z. Deng, M. Görner, and J. Zhang, "Object affordance based multimodal fusion for natural human-robot interaction," *Cogn. Syst. Res.*, pp. 128–137, 2019.
- [7] Y.-H. H. Tsai, S. Bai, P. P. Liang, J. Z. Kolter, L.-P. Morency, and R. Salakhutdinov, "Multimodal transformer for unaligned multimodal language sequences," in *Proc. Conf. Assoc. Comput. Linguistics*, 2019, p. 6558.
- [8] D. Hazarika, R. Zimmermann, and S. Poria, "Misa: Modality-invariant and-specific representations for multimodal sentiment analysis," in *Proc. of the 28th ACM Int. Conf. on Multimedia*, 2020, pp. 1122–1131.
- [9] W. Rahman, M. K. Hasan, S. Lee, A. Zadeh, C. Mao, L.-P. Morency, and E. Hoque, "Integrating multimodal information in large pretrained transformers," in *Proc. 58th Assoc. Comput. Linguistics*, 2020, p. 2359.
- [10] S. Huang, L. Qin, B. Wang, G. Tu, and R. Xu, "Sdif-da: A shallow-to-deep interaction framework with data augmentation for multi-modal intent detection," in *IEEE Int. Conf. Acoust., Speech Signal Process.*, 2024, pp. 10 206–10 210.
- [11] Q. Zhou, H. Xu, H. Li, H. Zhang, X. Zhang, Y. Wang, and K. Gao, "Token-level contrastive learning with modality-aware prompting for multimodal intent recognition," in *Proc. AAAI Conf. Artif. Intell.*, 2024, pp. 17 114–17 122.
- [12] H. Zhang, H. Xu, and T.-E. Lin, "Deep open intent classification with adaptive decision boundary," in *Proc. AAAI Conf. Artif. Intell.*, 2021, pp. 14 374–14 382.
- [13] H. Zhang, H. Xu, S. Zhao, and Q. Zhou, "Learning discriminative representations and decision boundaries for open intent detection," *IEEE/ACM Trans. Audio, Speech, and Lang. Process.*, pp. 1611–1623, 2023.
- [14] S. Larson, A. Mahendran, J. J. Peper, C. Clarke, A. Lee, P. Hill, J. K. Kummerfeld, K. Leach, M. A. Laurenzano, L. Tang, and J. Mars, "An evaluation dataset for intent classification and out-of-scope prediction," in *Proc. Conf. Empir. Methods Natural Lang. Process.*, 2019, pp. 1311–1316.
- [15] Y. C. Hsu, Y. Shen, H. Jin, and Z. Kira, "Generalized odin: Detecting out-of-distribution image without learning from out-of-distribution data," in *Proc. IEEE/CVF Conf. Comput. Vis. Pattern Recognit.*, 2020, pp. 10 948–10 957.
- [16] W. Liu, X. Wang, J. Owens, and Y. Li, "Energy-based out-of-distribution detection," in *Proc. Advances. Neural Inf. Process. Syst.*, vol. 33, 2020, pp. 21 464–21 475.
- [17] W. Zhou, F. Liu, and M. Chen, "Contrastive out-of-distribution detection for pretrained transformers," in *Proc. Conf. Empir. Methods Natural Lang. Process.*, 2021.
- [18] L.-M. Zhan, H. Liang, B. Liu, L. Fan, X.-M. Wu, and A. Y. Lam, "Out-of-scope intent detection with self-supervision and discriminative training," in *Proc. 59th Assoc. Comput. Linguistics*, 2021, pp. 3521–3532.
- [19] S. Esmailpour, B. Liu, E. Robertson, and L. Shu, "Zero-shot out-of-distribution detection based on the pre-trained model clip," in *Proc. AAAI Conf. Artif. Intell.*, 2022, pp. 6568–6576.
- [20] Y. Ming, Z. Cai, J. Gu, Y. Sun, W. Li, and Y. Li, "Delving into out-of-distribution detection with vision-language representations," *Proc. Advances. Neural Inf. Process. Syst.*, pp. 35 087–35 102, 2022.
- [21] L. Qin, T. Xie, W. Che, and T. Liu, "A survey on spoken language understanding: Recent advances and new frontiers," in *Proc. Int. Joint Conf. Artif. Intell.*, 2021, pp. 4577–4584.
- [22] A. Coucke, A. Saade, A. Ball, T. Bluche, A. Caulier, D. Leroy, C. Doumouro, T. Gisselbrecht, F. Caltagirone, T. Lavril *et al.*, "Snips voice platform: an embedded spoken language understanding system for private-by-design voice interfaces," *arXiv preprint arXiv:1805.10190*, 2018.
- [23] I. Casanueva, T. Temčinas, D. Gerz, M. Henderson, and I. Vulić, "Efficient intent detection with dual sentence encoders," in *Proc. 2nd Workshop Natural Lang. Process. Conversational AI*, 2020, pp. 38–45.
- [24] Q. Chen, Z. Zhuo, and W. Wang, "Bert for joint intent classification and slot filling," *arXiv preprint arXiv:1902.10909*, 2019.
- [25] W. He, Y. Dai, M. Yang, J. Sun, F. Huang, L. Si, and Y. Li, "Unified dialog model pre-training for task-oriented dialog understanding and generation," in *Proc. 45th Int. ACM SIGIR Conf. Res. Develop. Inf. Retrieval*, 2022, pp. 187–200.
- [26] Y. Zhou, P. Liu, and X. Qiu, "KNN-contrastive learning for out-of-domain intent classification," in *Proc. 60th Assoc. Comput. Linguistics*, 2022, pp. 5129–5141.
- [27] T.-E. Lin, H. Xu, and H. Zhang, "Discovering new intents via constrained deep adaptive clustering with cluster refinement," in *Proc. AAAI Conf. Artif. Intell.*, vol. 34, no. 05, 2020, pp. 8360–8367.

- [28] H. Zhang, H. Xu, T.-E. Lin, and R. Lyu, "Discovering new intents with deep aligned clustering," in *Proc. AAAI Conf. Artif. Intell.*, vol. 35, no. 16, 2021, pp. 14 365–14 373.
- [29] Y. Zhou, G. Quan, and X. Qiu, "A probabilistic framework for discovering new intents," in *Proc. 61st Assoc. Comput. Linguistics*, 2023, pp. 3771–3784.
- [30] H. Zhang, H. Xu, X. Wang, F. Long, and K. Gao, "A clustering framework for unsupervised and semi-supervised new intent discovery," *IEEE Trans. Knowl. Data Eng.*, 2023.
- [31] J. Kruk, J. Lubin, K. Sikka, X. Lin, D. Jurafsky, and A. Divakaran, "Integrating text and image: Determining multimodal document intent in instagram posts," *arXiv preprint arXiv:1904.09073*, 2019.
- [32] L. Zhang, J. Shen, J. Zhang, J. Xu, Z. Li, Y. Yao, and L. Yu, "Multimodal marketing intent analysis for effective targeted advertising," *IEEE Trans. Multimedia*, pp. 1830–1843, 2021.
- [33] G. V. Singh, M. Firdaus, A. Ekbal, and P. Bhattacharyya, "Emoint-trans: A multimodal transformer for identifying emotions and intents in social conversations," *IEEE/ACM Trans. Audio Speech Lang. Process.*, pp. 290–300, 2022.
- [34] M. Firdaus, H. Golchha, A. Ekbal, and P. Bhattacharyya, "A deep multi-task model for dialogue act classification, intent detection and slot filling," *Cogn. Computation*, pp. 626–645, 2021.
- [35] J. Godfrey, E. Holliman, and J. McDaniel, "Switchboard: telephone speech corpus for research and development," in *Proceedings of 1992 IEEE International Conference on Acoustics, Speech, and Signal Processing*, 1992, pp. 517–520 vol.1.
- [36] Y. Li, H. Su, X. Shen, W. Li, Z. Cao, and S. Niu, "Dailydialog: A manually labelled multi-turn dialogue dataset," *arXiv preprint arXiv:1710.03957*, 2017.
- [37] T. Saha, A. Patra, S. Saha, and P. Bhattacharyya, "Towards emotion-aided multi-modal dialogue act classification," in *Proc. 58th Assoc. Comput. Linguistics*, 2020, pp. 4361–4372.
- [38] S. Poria, D. Hazarika, N. Majumder, G. Naik, E. Cambria, and R. Mihalcea, "Meld: A multimodal multi-party dataset for emotion recognition in conversations," in *Proc. 57th Assoc. Comput. Linguistics*, 2019, pp. 527–536.
- [39] C. Busso, M. Bulut, C.-C. Lee, A. Kazemzadeh, E. Mower, S. Kim, J. N. Chang, S. Lee, and S. S. Narayanan, "Iemocap: Interactive emotional dyadic motion capture database," *Language Resour. Eval.*, pp. 335–359, 2008.
- [40] W. Yu, H. Xu, F. Meng, Y. Zhu, Y. Ma, J. Wu, J. Zou, and K. Yang, "Chsim: A chinese multimodal sentiment analysis dataset with fine-grained annotation of modality," in *Proc. 58th Assoc. Comput. Linguistics*, 2020, pp. 3718–3727.
- [41] A. Zadeh, R. Zellers, E. Pincus, and L.-P. Morency, "Mosi: multimodal corpus of sentiment intensity and subjectivity analysis in online opinion videos," *arXiv preprint arXiv:1606.06259*, 2016.
- [42] A. B. Zadeh, P. P. Liang, S. Poria, E. Cambria, and L.-P. Morency, "Multimodal language analysis in the wild: Cmu-mosei dataset and interpretable dynamic fusion graph," in *Proc. 56th Assoc. Comput. Linguistics*, 2018, pp. 2236–2246.
- [43] A. Zadeh, M. Chen, S. Poria, E. Cambria, and L.-P. Morency, "Tensor fusion network for multimodal sentiment analysis," in *Proc. Conf. Empir. Methods Natural Lang. Process.*, 2017, pp. 1103–1114.
- [44] Z. Liu, Y. Shen, V. B. Lakshminarasimhan, P. P. Liang, A. Bagher Zadeh, and L.-P. Morency, "Efficient low-rank multimodal fusion with modality-specific factors," in *Proc. 56th Assoc. Comput. Linguistics*, 2018, pp. 2247–2256.
- [45] A. Zadeh, P. P. Liang, N. Mazumder, S. Poria, E. Cambria, and L.-P. Morency, "Memory fusion network for multi-view sequential learning," in *Proc. AAAI Conf. Artif. Intell.*, 2018.
- [46] W. Han, H. Chen, and S. Poria, "Improving multimodal fusion with hierarchical mutual information maximization for multimodal sentiment analysis," in *Proc. Conf. Empirical Methods Natural Lang. Process.*, 2021, p. 9180–9192.
- [47] G. Hu, T.-E. Lin, Y. Zhao, G. Lu, Y. Wu, and Y. Li, "Unimse: Towards unified multimodal sentiment analysis and emotion recognition," in *Proc. Conf. Empir. Methods Natural Lang. Process.*, 2022, pp. 7837–7851.
- [48] C. Raffel, N. Shazeer, A. Roberts, K. Lee, S. Narang, M. Matena, Y. Zhou, W. Li, and P. J. Liu, "Exploring the limits of transfer learning with a unified text-to-text transformer," *J. Mach. Learn. Res.*, pp. 1–67, 2020.
- [49] Y. Zheng, G. Chen, and M. Huang, "Out-of-domain detection for natural language understanding in dialog systems," *IEEE/ACM Trans. Audio Speech Lang. Process.*, pp. 1198–1209, 2020.
- [50] B. Lee, J. Kim, J. Park, and K.-A. Sohn, "Improving unsupervised out-of-domain detection through pseudo labeling and learning," in *Findings Assoc. Comput. Linguistics: EACL 2023*, 2023, pp. 1031–1041.
- [51] Y. Shen, Y.-C. Hsu, A. Ray, and H. Jin, "Enhancing the generalization for intent classification and out-of-domain detection in slu," in *Proc. 59th Assoc. Comput. Linguistics*, 2021, pp. 2443–2453.
- [52] L.-M. Zhan, H. Liang, L. Fan, X.-M. Wu, and A. Y. Lam, "A closer look at few-shot out-of-distribution intent detection," in *Proc. 29th Int. Conf. Comput. Linguistics*, 2022, pp. 451–460.
- [53] K. Lee, K. Lee, H. Lee, and J. Shin, "A simple unified framework for detecting out-of-distribution samples and adversarial attacks," in *Proc. Advances. Neural Inf. Process. Syst.*, 2018, pp. 7166–7177.
- [54] I. Ndiour, N. Ahuja, and O. Tickoo, "Out-of-distribution detection with subspace techniques and probabilistic modeling of features," *arXiv preprint arXiv:2012.04250*, 2020.
- [55] H. Wang, Z. Li, L. Feng, and W. Zhang, "Vim: Out-of-distribution with virtual-logit matching," in *Proc. IEEE/CVF Conf. Comput. Vis. Pattern Recognit.*, 2022, pp. 4921–4930.
- [56] Z. Liu, Y. Lin, Y. Cao, H. Hu, Y. Wei, Z. Zhang, S. Lin, and B. Guo, "Swin transformer: Hierarchical vision transformer using shifted windows," in *Proc. IEEE Int. Conf. Comput. Vis.*, 2021, pp. 9992–10 002.
- [57] B. McFee, C. Raffel, D. Liang, D. P. Ellis, M. McVicar, E. Battenberg, and O. Nieto, "librosa: Audio and music signal analysis in python," in *Proc. 14th Python Sci. Conf.*, 2015, pp. 18–25.
- [58] S. Chen, C. Wang, Z. Chen, Y. Wu, S. Liu, Z. Chen, J. Li, N. Kanda, T. Yoshioka, X. Xiao *et al.*, "Wavlm: Large-scale self-supervised pre-training for full stack speech processing," *IEEE J. Sel. Topics Signal Process.*, pp. 1505–1518, 2022.
- [59] Y. Ouyang, J. Ye, Y. Chen, X. Dai, S. Huang, and J. Chen, "Energy-based unknown intent detection with data manipulation," in *Findings Assoc. Comput. Linguistics: ACL-IJCNLP 2021*, 2021, pp. 2852–2861.
- [60] Z. Cheng, Z. Jiang, Y. Yin, C. Wang, and Q. Gu, "Learning to classify open intent via soft labeling and manifold mixup," *IEEE/ACM Trans. Audio, Speech, and Lang. Process.*, vol. 30, pp. 635–645, 2022.
- [61] J. D. M.-W. C. Kenton and L. K. Toutanova, "Bert: Pre-training of deep bidirectional transformers for language understanding," in *Proc. North Amer. Chapter Assoc. Comput. Linguistics: Hum. Lang. Technol.*, 2019, pp. 4171–4186.
- [62] A. Vaswani, N. Shazeer, N. Parmar, J. Uszkoreit, L. Jones, A. N. Gomez, E. Kaiser, and I. Polosukhin, "Attention is all you need," in *Proc. Int. Conf. Neural Inf. Process. Syst.*, vol. 30, 2017.
- [63] J. Yang, K. Zhou, Y. Li, and Z. Liu, "Generalized out-of-distribution detection: A survey," *Int. Journal of Comput. Vis.*, pp. 1–28, 2024.
- [64] P. Wang, K. He, Y. Mou, X. Song, Y. Wu, J. Wang, Y. Xian, X. Cai, and W. Xu, "App: Adaptive prototypical pseudo-labeling for few-shot ood detection," in *Findings Assoc. Comput. Linguistics: EMNLP 2023*, 2023, pp. 3926–3939.
- [65] J. Tian, Y.-C. Liu, N. Glaser, Y.-C. Hsu, and Z. Kira, "Posterior recalibration for imbalanced datasets," in *Proc. Int. Conf. Neural Inf. Process. Syst.*, 2020, pp. 8101–8113.
- [66] H. Qi, M. Brown, and D. G. Lowe, "Low-shot learning with imprinted weights," in *Proc. IEEE/CVF Conf. Comput. Vis. Pattern Recognit.*, 2018, pp. 5822–5830.
- [67] T. Gao, X. Yao, and D. Chen, "Simcse: Simple contrastive learning of sentence embeddings," in *Proc. Conf. Empir. Methods Natural Lang. Process.*, 2021, pp. 6894–6910.
- [68] A. Stolcke, K. Ries, N. Coccaro, E. Shriberg, R. Bates, D. Jurafsky, P. Taylor, R. Martin, C. V. Ess-Dykema, and M. Meteer, "Dialogue act modeling for automatic tagging and recognition of conversational speech," *Comput. Linguistics*, pp. 339–373, 2000.
- [69] D. Hendrycks and K. Gimpel, "A baseline for detecting misclassified and out-of-distribution examples in neural networks," in *Proc. Int. Conf. Learn. Representations*, 2017.
- [70] S. Liang, Y. Li, and R. Srikant, "Enhancing the reliability of out-of-distribution image detection in neural networks," in *Proc. Int. Conf. Learn. Representations*, 2018.
- [71] T. Yu, H. Gao, T.-E. Lin, M. Yang, Y. Wu, W. Ma, C. Wang, F. Huang, and Y. Li, "Speech-text pre-training for spoken dialog understanding with explicit cross-modal alignment," in *Proc. 61st Assoc. Comput. Linguistics*, 2023, pp. 7900–7913.
- [72] A. v. d. Oord, Y. Li, and O. Vinyals, "Representation learning with contrastive predictive coding," *arXiv preprint arXiv:1807.03748*, 2018.
- [73] S. Ryu, S. Koo, H. Yu, and G. G. Lee, "Out-of-domain detection based on generative adversarial network," in *Proc. Conf. Empir. Methods Natural Lang. Process.*, 2018, pp. 714–718.

- [74] T. Wolf, L. Debut, V. Sanh, J. Chaumond, C. Delangue, A. Moi, P. Cistac, T. Rault, R. Louf, M. Funtowicz *et al.*, “Transformers: State-of-the-art natural language processing,” in *Proc. Conf. Empir. Methods Natural Lang. Process.*, 2020, pp. 38–45.
- [75] I. Loshchilov and F. Hutter, “Decoupled weight decay regularization,” in *Proc. Int. Conf. Learn. Representations*, 2019.
- [76] A. Zaemzadeh, N. Bisagno, Z. Sambugaro, N. Conci, N. Rahnavard, and M. Shah, “Out-of-distribution detection using union of 1-dimensional subspaces,” in *Proc. IEEE/CVF Conf. Comput. Vis. Pattern Recognit.*, 2021, pp. 9452–9461.